Exploring the superfocusing performance of plasmonic lenses formed by coupled nanoslits

Yechuan Zhu[1,2], Weizheng Yuan[1,2], Yiting Yu[1,2] ✉, Ping Wang[1,2], Hao Sun[1,2]

[1]*Key Laboratory of Micro/Nano Systems for Aerospace, Ministry of Education, Northwestern Polytechnical University, Xi'an 710072, People's Republic of China*
[2]*Key Laboratory of Micro- and Nano-Electro-Mechanical Systems of Shaanxi Province, Northwestern Polytechnical University, Xi'an 710072, People's Republic of China*
✉ *E-mail: yyt@nwpu.edu.cn*

Published in Micro & Nano Letters; Received on 12th May 2016; Accepted on 16th August 2016

A comprehensive investigation on the superfocusing performance of a plasmonic lens formed by coupled metallic nanoslits is carried out. Based on the geometrical optics and the wavefront reconstruction principle, the nanoslit array for a plasmonic lens is optimally designed to achieve the desired phase modulation by considering the influence of the coupling between adjacent aperiodic nanoslits on phase delay and the theory of periodic metallic nanoslits. The designed lens' focusing behaviour is verified by using the finite-difference time-domain method. Numerical results demonstrate that the superfocusing performance of a plasmonic lens has a close relationship with the lens size, focal length, working medium and incident wavelength. A larger lens size, a shorter focal length, a higher-index working medium can contribute to producing a higher-resolution superfocusing. Moreover, due to the material response, a shorter wavelength is not beneficial for an efficient focusing.

1. Introduction: Miniaturised optical lenses with high efficiency are of great significance for the highly integrated photonic circuits [1]. However, when the conventional refractive lenses are used to focus light, the focusing performance deteriorates as their sizes approach the operating wavelength. In addition, the resolution is generally restricted to $\lambda/2$ (λ is the operating wavelength) due to the diffraction limit. By utilising the surface plasmon polaritons (SPPs), metallic planar lenses illustrate tremendous promise for overcoming this resolution limit, which have potential applications in highly integrated optics, lithography and super-resolution imaging [2]. Remarkably, a resolution of $\lambda/6$ was realised by a metallic slab superlens [3]. Nevertheless, the object and image are limited in the near field, only tens of nanometres away from the superlens. Recently, metallic lenses made of various nanostructures such as slits, apertures, holes and surface corrugations, have been developed to achieve the light focusing covering a larger distance [4–9].

Using the width and position of a metal nanoslit to manipulate optical phase delay, plasmonic lenses formed by metal nanoslit arrays have been investigated both numerically [10–12] and experimentally [13–15]. In comparison with the metallic slab superlens, this type of metallic nanostructured lenses can realise the focusing at an anticipated distance from the lens via the proper structural design. Nevertheless, in these previous studies, few could break the diffraction limit. Furthermore, metallic spacing larger than twice the skin depth is employed in these designed lenses to decouple the SPPs propagating in any two adjacent nanoslits, which leads to a low transmission efficiency. In our recent research, a planar plasmonic lens consisting of coupled nanoslits with the spacings smaller than twice the skin depth is constructed, and it can well break the diffraction limit [16]. Here, based on our previous work [17], we comprehensively investigate the influence of main factors such as the lens size, the focal length, the working medium and incident wavelength on the superfocusing performance of the plasmonic lens.

2. Design of superfocusing plasmonic lenses: Fig. 1 shows the schematic focusing of the plasmonic lens consisting of a series of coupled nanoslits perforated in a gold film on a glass substrate. The lens working in a dielectric is symmetric with respect to the plane $y = 0$. When a TM-polarised plane wave is incident on the lens, the SPPs can be excited at the nanoslit entrance and propagate inside the nanoslits in the TM modes. Then, they radiate into the working dielectric. The focusing with the desired focal length f can be realised, provided that the phase delay of each nanoslit matches the required phase difference ($\Delta\varphi(y) - \Delta\varphi(0)$) as a function of the position y, which can be calculated by

$$\Delta\varphi(y) - \Delta\varphi(0) = 2m\pi + \frac{2\pi n_{\mathrm{d}} f}{\lambda} - \frac{2\pi n_{\mathrm{d}}\sqrt{f^2 + y^2}}{\lambda} \quad (1)$$

where λ is the free-space wavelength, m is an arbitrary integer and n_{d} is the refractive index of the working dielectric for the lens. Therefore, the phase delay of each nanoslit is the key point for designing the metallic planar lens.

We first investigate the influence of the refractive index of working medium on the focusing performance of the plamonic lens. Three different refractive indices of $n_{\mathrm{d}} = 1$, 1.5, 2 are considered here. The same procedure as reported in [16] is taken for designing our lenses. The plasmonic lenses working in different refractive-index dielectrics with the designed focal length of 0.3 μm are constructed based on the metallic spacing of 30 nm in a 400 nm thick gold film. On the one hand, the phase delay of a coupled nanoslit filled with the different index dielectrics depends on its own width, the width of adjacent ones and the metallic spacings between them, similar to the situation which was investigated in detail in [16]. On the other hand, it is also related to the refractive index of the filling dielectric. When the influence of the aperiodicity of adjacent nanoslits on the phase delay is small, the phase delay of a coupled nanoslit can be effectively predicted by $\mathrm{Re}(\beta)t$, where t is the thickness of the metal film and β is the complex propagation constant in the nanoslit which is calculated based on the symmetric-mode dispersion relation in a periodic metallic nanoslit array with the following equation [18]

$$\cos(wk_1)\cos(sk_2) - \frac{\varepsilon_m^2 k_1^2 + k_2^2}{2\varepsilon_m k_1 k_2}\sin(wk_1)\sin(sk_2) = 1. \quad (2)$$

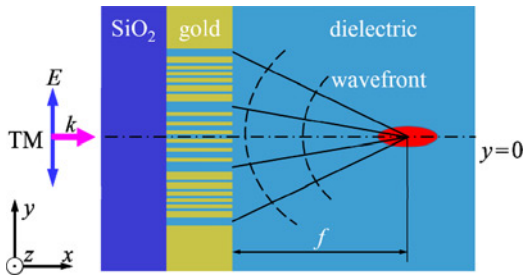

Fig. 1 *Schematic focusing of a metallic nanoslit-based plasmonic lens located on a glass substrate and working in a dielectric*

where $k_1 = (\varepsilon_d k^2 - \beta^2)^{1/2}$ and $k_2 = (\varepsilon_m k^2 - \beta^2)^{1/2}$. Here, w is the nanoslit width. s is the spacing between adjacent nanoslits. k is the free-space wavevector. ε_m and ε_d are the permittivity of the metal and dielectric material inside the nanoslits, respectively. At the working wavelength of $\lambda = 650$ nm, ε_m is $-12.8915 + 1.2044i$ for gold [19]. For the specific spacing of $s = 30$ nm and 400 nm thick gold film, on the basis of (2), the dependence of phase delay on the nanoslit width when these nanoslits are immersed in the dielectric with $n_d = 1$, 1.5, 2 is shown in Fig. 2. We can observe that compared with the filling of the dielectric with $n_d = 1$, a much larger varying range of the phase delay can be obtained through the filling of a high-index dielectric. For example, as the nanoslit width increases from 10 to 60 nm, the phase delay of a nanoslit filled with the dielectric of $n_d = 1$, decreases from 2.65π to 1.51π, while it varies from 8.03π to 3.23π when the refractive index of the filling dielectric is $n_d = 2$. The modulation range of the phase delay for the latter is more than four times as large as that of the former. It implies that the narrowest nanoslit constructing a metallic planar lens working in a high-index dielectric can be broadened. On the other hand, the wider nanoslit is beneficial for improving the optical transmission efficiency and alleviating the practical nanofabrication of the device. Therefore, the filling of a high-index dielectric is beneficial for lens focusing and nanofabrication.

Combining the theoretical calculation based on (1) and (2) with the influence of the coupling between aperiodic nanoslits on the phase delay, the metallic lenses working in the dielectric of $n_d = 1$, 1.5, 2 are optimally designed with a total phase difference $(\Delta\varphi(y) - \Delta\varphi(0))$ of 2π for the desired focal length of 0.3 μm, as shown in Fig. 3. The width of the narrowest nanoslit is 10 nm for the lens working in the dielectric of $n_d = 1$, but changed to 22 and

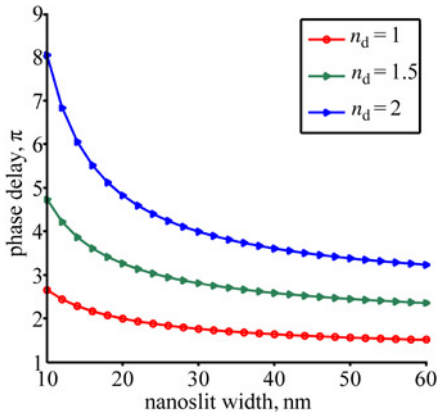

Fig. 2 *Dependence of phase delay on the nanoslit width introduced by a coupled nanoslit filled with dielectrics of different refractive indices, which is analysed based on (2). Refractive index of the filling dielectric is 1, 1.5, 2, respectively. Gold spacing between two adjacent nanoslits is 30 nm, and the thickness of the gold film is 400 nm*

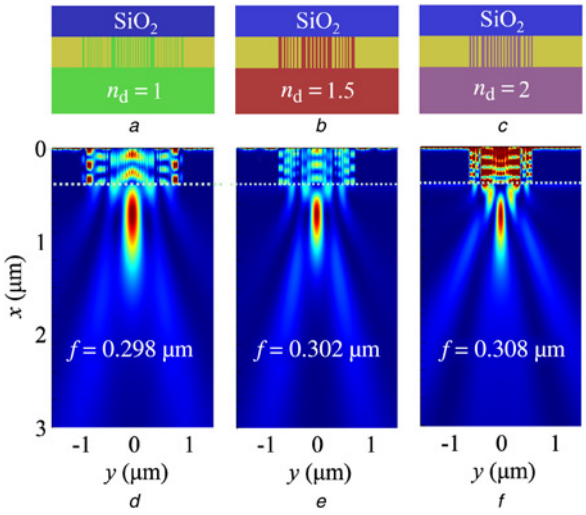

Fig. 3 *Optimised plasmonic lenses working in three different refractive-index dielectrics for the designed focal length of 0.3 μm at a wavelength of 650 nm*
a Lens working in the dielectric of $n_d = 1$ taken from [16]
b Lens working in the dielectric of $n_d = 1.5$. Beginning from $y = 0$, the width sequences of nanoslits are: 38, 40, 48, 82, 22, 22, 22, 22, 26, 60 nm and the corresponding spacing sequences of gold walls are: 30, 30, 30, 60, 46, 36, 32, 30, 40 nm
c Lens working in the dielectric of $n_d = 2$. Beginning from $y = 0$, the width sequences of nanoslits are: 28, 28, 30, 34, 42, 60, 30, 30, 30 nm and the corresponding spacing sequences of gold walls are: 30, 30, 30, 30, 30, 58, 40, 30 nm. The simulated magnetic-field intensity for lenses working in the dielectric with
d $n_d = 1$
e $n_d = 1.5$
f $n_d = 2$. White dashed lines denote the exit surface of the lenses

28 nm when the lens works in the dielectric of $n_d = 1.5$, 2, respectively, as a result of the filling of high-index dielectric in the nanoslits, which is consistent with the above analysis.

Our designs are validated by the full electromagnetic field simulations using the finite-difference time-domain (FDTD) method. In simulations, perfectly matched layers as the absorbing boundary conditions are employed around the computational domain. The incident TM-polarised plane wave is defined by setting the electric field component of E_y with the amplitude equal to 1.

Fig. 3 gives the calculated magnetic-field intensity for the plasmonic lenses working in the dielectric of $n_d = 1$, 1.5, 2. From the numerical results, it can be obviously observed that the design for a plasmonic lens is verified, since the simulated focal lengths of plasmonic lenses all agree well with the anticipated ones. Meanwhile, as compared with the lens operating in the dielectric of $n_d = 1$, the lenses working in high-index dielectrics have a more confined light focusing capability. The detailed focusing performance for the lenses operating in the dielectric of $n_d = 1$, 1.5, 2 is given in Table 1. We can see that a plasmonic lens working in a higher-index dielectric has a smaller full width at half maximum (FWHM). However, the variation of the focal spot's peak intensity as the refractive index of working dielectric is a little complicated,

Table 1 Derived focusing performance for the designed lenses working in different refractive-index dielectrics

Refractive index of dielectric	Lens aperture, μm	FWHM, nm	Max. intensity, a.u.
1	1.852	250 (λ/2.60)	2.6844
1.5	1.394	176 (λ/3.69)	3.7678
2	1.152	134 (λ/4.85)	1.2994

doi: 10.1049/mnl.2016.0288

which increases firstly and then decreases with the increasing refractive index. The underlying physical mechanism is that the filling of the working dielectric with the refractive index above a certain value can disrupt the coupled mode of the SPPs in the nanoslits, which thus causes more losses when the light is transmitted through the nanoslits.

Furthermore, the superfocusing performance of a plamonic lens is closely related with the lens size. Taking the above lens working in the dielectric of $n_d = 1.5$ as an example, lenses with different apertures are built and the focusing behaviour is validated using the method of FDTD. The simulated focusing performance is shown in Fig. 4. Similar to the conventional refractive lenses, the focusing resolution and peak light intensity of a plasmonic lens increase with the lens aperture. In addition, we note that the lens with an aperture size of 3.23 μm can realise a superfocusing of 148 nm, i.e. $\lambda/4.39$, showing a better result than the achieved resolution of $\lambda/3.46$ for a super-oscillatory lens with an extremely large lens size of 40 μm [20].

On the other hand, the position of the focal spot has a strong influence on the ultimate focusing performance of a plasmonic lens. Here, plasmonic lenses working in the dielectric of $n_d = 1$ with various focal lengths at a wavelength of 650 nm are designed. Fig. 5 demonstrates the calculated FWHM of a focal spot as a function of the lens' focal length. It can be found that the superfocusing capability of a plasmonic lens becomes worse when the lens focuses light at a farther distance. Therefore, in order to achieve the superfocusing performance, the anticipated focal length of a plasmonic lens should not be too large.

Due to the dispersion properties of metal materials, the incident wavelength also affects greatly the focusing behaviour of a plasmonic lens formed by coupled nanoslits perforated in a metal film. As a comparison, a shorter wavelength of 405 nm is selected. At this wavelength, ε_m is $-1.6745 + 5.7286i$ for gold [19], whose imaginary part is much bigger than that for gold at 650 nm, implying a greater loss in the structure. Fig. 6 shows the focusing performance of two plasmonic lenses working at different wavelengths with an anticipated focal length of 0.3 μm. The peak intensity of the focal spot for the lens at 405 nm is even smaller than one-tenth of that for the lens at 650 nm, although the two lenses have nearly the same aperture. This is because a shorter wavelength leads to a greater loss when the light propagates in the nanoslits, which can be obviously seen from the magnetic-field intensity distribution in the nanoslits. Meanwhile, an obvious focal shift occurs at the shorter wavelength.

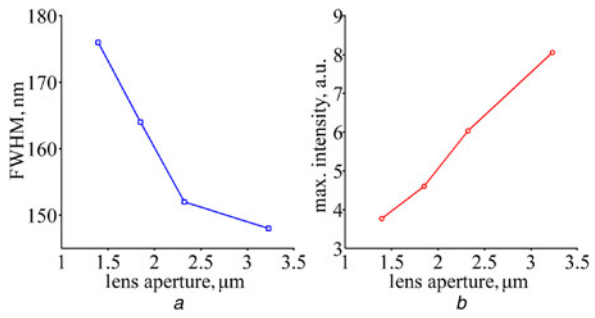

Fig. 4 *Effect of the lens size on the focusing performance of a plasmonic lens*
a Effect of the lens size on the focal spot size
b Effect of the lens size on the light intensity

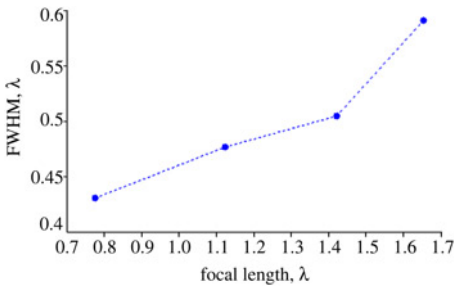

Fig. 5 *Effect of the focal length on the FWHM of the focusing spot of a plasmonic lens with the total phase difference of 2π. λ is the incident wavelength (650 nm)*

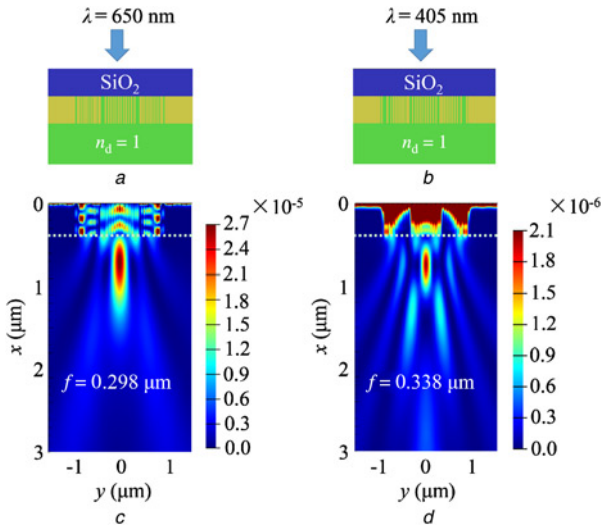

Fig. 6 *Focusing performance of plasmonic lenses operating at different wavelengths with the designed focal length of 0.3 μm*
a Lens operating at 650 nm taken from [16]
b Lens operating at 405 nm. Beginning from $y = 0$ (the centre of the lens), the width sequences of nanoslits are: 20, 20, 22, 26, 32, 50, 10, 10, 10, 12, 14, 18, 24, 38, 80,10 nm and the corresponding spacing sequences of gold walls are: 30, 30, 30, 30, 30, 80, 42, 34, 30, 30, 30, 30, 30, 40, 36 nm. The simulated magnetic-field intensity for lenses operating at
c $\lambda = 650$ nm
d $\lambda = 405$ nm. White dashed lines denote the exit surface of the plasmonic lenses

3. Conclusions: To sum up, based on the special propagating properties of the SPPs in coupled nanoslits, a series of plasmonic lenses consisting of coupled nanoslits perforated in a gold film are optimally designed, which are fully validated by the numerical simulation using the FDTD method. According to the simulation results, the influence of refractive index of the working dielectric, the lens size, the focal length, and the incident wavelength on the focusing performance of a plasmonic lens is investigated in detail. We conclude that a higher-index working medium, a larger lens size and a shorter focusing distance can all contribute to the higher-resolution superfocusing. Moreover, the shorter wavelength and the working dielectric with a refractive index above a certain value can result in the focusing with lower efficiency due to the loss in the structures. Therefore, in order to achieve the desired focusing performance, one must take all these factors into account.

4. Acknowledgments: This work was supported by National Natural Science Foundation of China (grant no. 51375400); Fundamental Research Funds for the Central Universities (grant no. 3102014JC02020504); the Specific Project for the National Excellent Doctorial Dissertations (grant no. 201430); the Program for the New Century Excellent Talents in University; and Innovation Foundation for Doctor Dissertation of Northwestern Polytechnical University.

5 References

[1] Chen J., Li Z., Zhang X., *ET AL.*: 'Submicron bidirectional all-optical plasmonic switches', *Sci. Rep.*, 2013, **3**, p. 1451

[2] Barnes W.L., Dereux A., Ebbesen T.W.: 'Surface plasmon subwavelength optics', *Nature*, 2003, **424**, pp. 824–830

[3] Zhang X., Liu Z.: 'Superlenses to overcome the diffraction limit', *Nat. Mater.*, 2008, **7**, pp. 435–441

[4] Garcia-Vidal F.J., Martin-Moreno L., Lezec H.J., *ET AL.*: 'Focusing light with a single subwavelength aperture flanked by surface corrugations', *Appl. Phys. Lett.*, 2003, **83**, p. 4500

[5] Lin L., Goh X.M., McGuinness L.P., *ET AL.*: 'Plasmonic lenses formed by two-dimensional nanometric cross-shaped aperture arrays for Fresnel-region focusing', *Nano Lett.*, 2010, **10**, pp. 1936–1940

[6] Kawata S., Inouye Y., Verma P.: 'Plasmonics for near-field nano-imaging and superlensing', *Nat. Photonics*, 2009, **3**, pp. 388–394

[7] Liu Z., Durant S., Lee H., *ET AL.*: 'Far-field optical superlens', *Nano Lett.*, 2007, **7**, (2), pp. 403–408

[8] Fu Y., Mote R.G., Wang Q., *ET AL.*: 'Experimental study of plasmonic structures with variant periods for sub-wavelength focusing: analyses of characterization errors', *J. Mod. Opt.*, 2009, **56**, pp. 1550–1556

[9] Gao H., Hyun J.K., Lee M.H., *ET AL.*: 'Adband plasmonic microlenses based on patches of nanoholes', *Nano Lett.*, 2010, **10**, (10), pp. 4111–4116

[10] Yu Y., Zappe H.: 'Effect of lens size on the focusing performance of plasmonic lenses and suggestions for the design', *Opt. Express*, 2011, **19**, (10), pp. 9434–9444

[11] Yu Y., Zappe H.: 'Theory and implementation of focal shift plasmonic of lenses', *Opt. Lett.*, 2012, **37**, (9), pp. 1592–1594

[12] Shi H., Wang C., Du C., *ET AL.*: 'Beam manipulating by metallic nanoslits with variant widths', *Opt. Express*, 2005, **13**, (18), pp. 6815–6820

[13] Verslegers L., Catrysse P.B., Yu Z., *ET AL.*: 'Planar lenses based on nanoscale slit arrays in a metallic film', *Nano Lett.*, 2009, **9**, (1), pp. 235–238

[14] Chen Q., Cumming D.R.S.: 'Visible light focusing demonstrated by plasmonic lenses based on nano-slits in an aluminum film', *Opt. Express*, 2010, **18**, (14), pp. 14788–14793

[15] Ishii S., Kildishev A.V., Shalaev V.M., *ET AL.*: 'Metal nanoslit lenses with polarization-selective design', *Opt. Lett.*, 2011, **36**, (4), pp. 451–453

[16] Zhu Y., Yuan W., Yu Y., *ET AL.*: 'Metallic planar lens formed by coupled width-variable nanoslits for superfocusing', *Opt. Express*, 2015, **23**, (15), pp. 20124–20131

[17] Zhu Y., Yuan W., Yu Y., *ET AL.*: 'Superfocusing properties of metallic planar lens based on coupled width-variable nanoslits'. The 11th IEEE Int. Conf. on Nano/Micro Engineered and Molecular Systems (NEMS), Matsushima Bay and Sendai MEMS City, Japan, 2016

[18] Verslegers L., Catrysse P.B., Yu Z., *ET AL.*: 'Planar metallic nanoscale slit lenses for angle compensation', *Appl. Phys. Lett.*, 2009, **95**, (7), p. 071112

[19] Johnson P.B., Christy R.W.: 'Optical constants of the noble metals', *Phys. Rev. B*, 1972, **6**, (12), pp. 4370–4379

[20] Rogers E.T.F., Lindberg J., Roy T., *ET AL.*: 'A super-oscillatory lens optical microscope for subwavelength imaging', *Nat. Mater.*, 2012, **11**, (5), pp. 432–435

doi: 10.1049/mnl.2016.0288